Technical Note

1977-10

The Firepond Kalman Filter

S. F. Catalano

4 February 1977

Prepared for the Defense Advanced Research Projects Agency
under Electronic Systems Division Contract F19628-76-C-0002 by

Lincoln Laboratory

MASSACHUSETTS INSTITUTE OF TECHNOLOGY

LEXINGTON, MASSACHUSETTS

The work reported in this document was performed at Lincoln Laboratory, a center for research operated by Massachusetts Institute of Technology. This work was sponsored by the Defense Advanced Research Projects Agency under Air Force Contract F19628-76-C-0002 (ARPA Order 600).

This technical report has been reviewed and is approved for publication.

FOR THE COMMANDER

Raymond L. Loiselle

Raymond L. Loiselle, Lt. Col., USAF
Chief, ESD Lincoln Laboratory Project Office

MASSACHUSETTS INSTITUTE OF TECHNOLOGY
LINCOLN LABORATORY

THE FIREPOND KALMAN FILTER

S. F. CATALANO
Group 54

TECHNICAL NOTE 1977-10

4 FEBRUARY 1977

LEXINGTON MASSACHUSETTS

ABSTRACT

This report describes the satellite tracking Kalman filter implemented at the M.I.T. Lincoln Laboratory Firepond Infrared Research Facility at Westford, MA. The filter estimates a six dimensional state vector for mount direction from satellite observations. These observations can consist of range, elevation, azimuth, and range rate; and under push-button control, can be selected from among the available Firepond detectors (IR and optical) and the Millstone radar across the road.

Radar polar coordinates are used throughout and, in particular, both the estimates and the equations of motion are in these coordinates. The filter is fully coupled in the sense that every measurement improves every estimate. For example, angle measurements improve range and Doppler estimates, and conversely. Serial processing of simultaneous measurements is employed. This eliminates the need for matrix inversion, facilitates handling of missing data points, requires less storage, and is computationally faster.

A detailed mathematical description of the filter is included along with some typical satellite tracking results.

CONTENTS

I. INTRODUCTION

A Kalman filter for satellite direction has been designed, implemented, and in routine mission operation at the M.I.T. Lincoln Laboratory Firepond Infrared Research Facility in Westford, Mass. The filter accepts pre-smoothed observations every tenth second and estimates an improved state vector from a predicted state vector and these observations. The predicted state vector is based on the equations of motion. Radar polar coordinates are used throughout and the state vector is six dimensional with components R, E, A, $\dot{R}$, $\dot{E}$, $\dot{A}$ (range, elevation, azimuth, and their rates respectively). The observation vector can be up to four dimensional with components R, E, A, $\dot{R}$. These components are processed sequentially, with time increment $\Delta t = 0$. This facilitates the handling of bad or missing data points and avoids matrix inversion. Under push-button control, the four (or less) observation components can be selected from the following data sources:

a. Millstone R, E, A, $\dot{R}$

b. upper visible E, A

c. lower visible E, A

d. IR R, E, A, $\dot{R}$

These can be mixed in any way with the exception that both angles must be from one source. For example, the filter can accept Millstone range, lower visible angles, and IR Doppler. If no observations are selected or available, the filter does a predict (i.e., coast) cycle without estimation. The filter is fully coupled in the sense that every measurement component improves the estimation of every state vector component. For example, angle measurements improve range and Doppler estimates, and conversely.

All known biases (mount misalignment, refraction, etc.) are removed from

observations before input to the Kalman filter. Based on these true observations the filter estimates a state vector, extrapolates it to the next tenth second, again accounts for biases, and makes available a predicted state vector which, at the option of the test director, can be used to direct the mount. The Kalman track residuals are displayed (CRT) and recorded (strip chart) for real-time viewing to help judge the quality of the Kalman track. The observations and filter estimates are also recorded on magnetic tape for post-mission analysis.

The filter has been successfully used in a variety of missions. Some typical results are shown in Section IV.

II. PREPROCESSOR

1. Firepond Data

The function of the Firepond data preprocessor is to reduce data rates to something the Kalman filter can handle in the available time. Recursive linear least squares smoothing is performed on data between tenth second markers. Smoothed values are updated to make them valid at the tenth second markers on or immediately following the last sample in the smoothing interval. The smoothing algorithm used is that due to N. Levine reported in Ref. 5 and, as herein applied, assumes equally-spaced, equally-weighted samples.

The data samples fed to this smoothing algorithm are formed as indicated below and the smoothing algorithm itself is outlined in Appendix D.

a. Range

An algorithm which computes range track offsets from early/late gate values resides in the real time program but is not presently used. Instead, uncorrected range encoder values at the PRI rate (250 pps maximum) are smoothed, updated, converted to meters, and fed to the Kalman filter every tenth second.

b. Range Rate

Doppler synthesizer frequencies and filter bank Doppler offsets are available at the PRI rate. These are combined, smoothed, updated, corrected for relativistic and refraction effects, converted to m/sec, and fed to the Kalman filter every tenth second.

c. Angles

The 50 pps angle track error components, according to tracker type, are indicated below.

Tracker	Error Components, 50 pps
IR	Monopulse, scan mirror, transit time mirror
Lower Visible	LV detector, scan mirror, transit time mirror
Upper Visible	UV detector

The error components for the selected tracker are combined, smoothed, updated, and added to refraction corrected angle encoder values at the tenth second level. In the case of the lower visible tracker, the incremental refraction mirror correction is also added at the tenth second level. The results are converted to radians and fed to the Kalman filter every tenth second.

d. Updating

The tenth-second updating is done after the data samples are formed and smoothed as indicated above. Smoothed values, X, are linearly extrapolated to the next tenth second (indicated by the subscript ten) as:

$$X_{10} = X + \dot{X}\Delta T \quad .$$

The rates $\dot{X}$ are approximated from the Kalman filter estimated rates at the previous tenth second. The time increments ΔT are indicated below for R, E, A, and $\dot{R}$.

$$\Delta T_R = \Delta t - R/C$$

$$\Delta T_E,\ \Delta T_A = \Delta t + R/C \text{ for upper visible}$$

$$= \Delta t + 2R/C \text{ for lower visible and IR}$$

$$\Delta T_{\dot{R}} = \Delta t - R/C + PRI$$

where Δt = time between last datum in the smoothing interval and the next even tenth second

R/C = transit time to target

PRI = one pulse repetition interval

The transit time and PRI terms are required by the hardware to make the samples valid at target illumination time.

2. Millstone Data

The Millstone radar observations (R_M, E_M, A_M, $\dot{R}_M$) are fully corrected and are available at 15 pps. These are reduced to 10 pps by accepting data only at the last time in a tenth second interval. These are then referenced to Firepond and fed to the Kalman filter every tenth second.

The positional components (R_M, E_M, A_M) are first put in radar rectangular coordinates (X_M, Y_M, Z_M) and then converted to Firepond rectangular coordinates by the usual rotation and translation.

$$\begin{bmatrix} X_F \\ Y_F \\ Z_F \end{bmatrix} = [A] \begin{bmatrix} X_M \\ Y_M \\ Z_M \end{bmatrix} + \begin{bmatrix} B_X \\ B_Y \\ B_Z \end{bmatrix}$$

The rotation matrix [A] is prestored in the real time program. The translation vector (B_X, B_Y, B_Z) is also prestored (but with opposite sign sense). The Firepond-

referenced rectangular components are then put in Firepond polar coordinates (R, E, A).

The range rate component $\dot{R}_M$ is referenced to Firepond as indicated in Appendiz E. The transformation of the associated measurement accuracy weightings to Firepond coordinates is neglected since the sites are so close.

III. THE KALMAN FILTER

1. Introduction

Included herein is a mathematical description of the Kalman filter as it is presently implemented on the Real Time Program at Firepond. The filter algorithm is a modification and extension of that described in Reference 1. The block diagram in Figure 1 presents a convenient overview of the whole process. This is followed by a description of each step in more mathematical detail.

The input observations to the filter consist of the tenth-second smoothed and corrected R, E, A, and $\dot{R}$ samples. Also required are the covariance matrix M of these measurements, an initial state vector and its covariance matrix. The algorithm then consists of a process of prediction and estimation as indicated in Figure 1. At each point in time the estimation requires a predicted state vector (and its convariance matrix) along with an observation vector, while the prediction requires an estimate of the last state vector (and its covariance matrix) and the equations of motion.

State vector estimates are converted to Cartesian coordinates and placed in the RTP target file for possible laser mount directing.

2. Equations of Motion

The equations of motion in radar polar coordinates are shown in Appendix A. They appear therein as three coupled second order differential equations. These

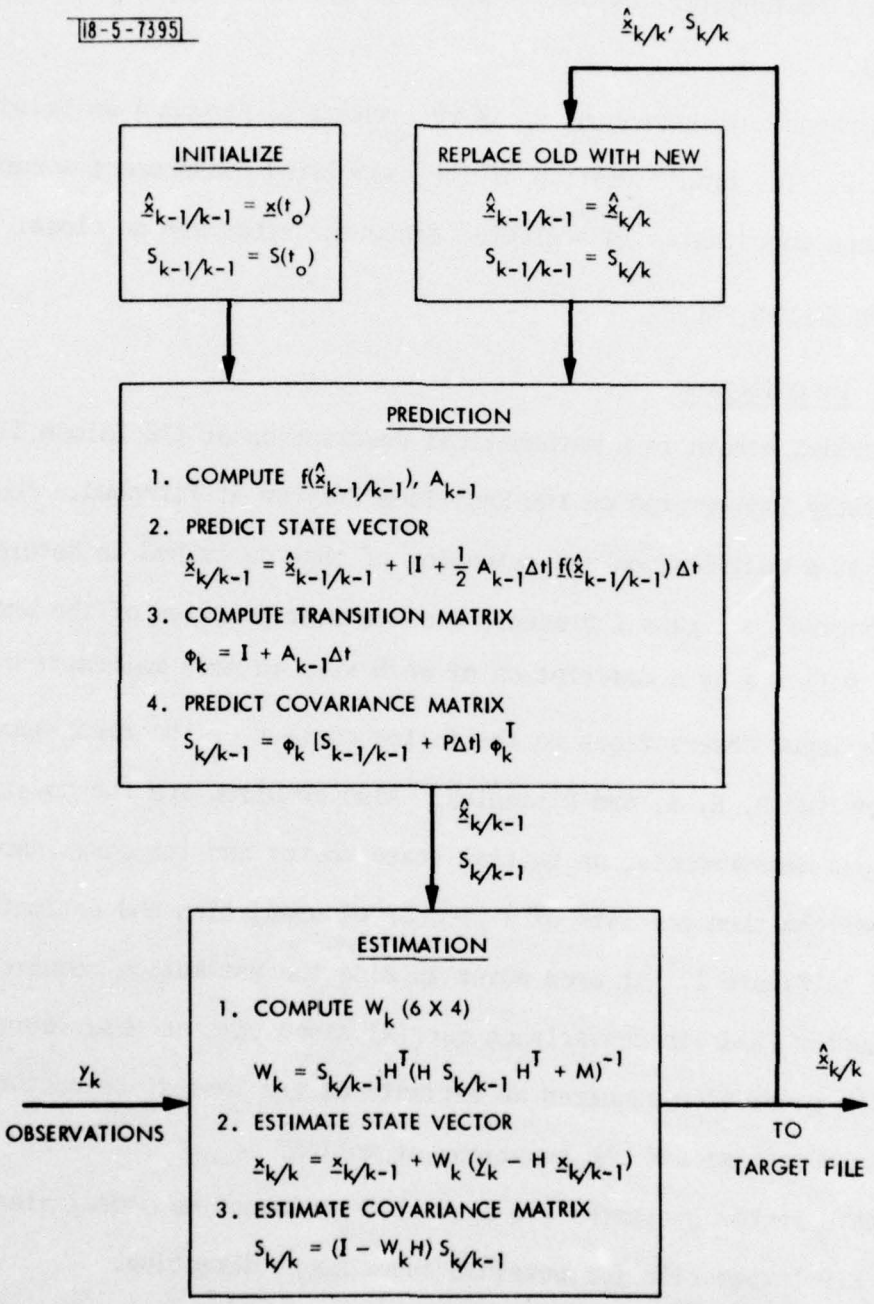

Fig. 1. Firepond Kalman Filter.

can be compactly written as the first order vector differential equation

$$\dot{\underline{x}} = \underline{f}(\underline{x}), \quad \underline{x}(t_o) = \underline{x}_o \tag{1}$$

where $\underline{x}$ is the state vector with components R, E, A, $\dot{R}$, $\dot{E}$, $\dot{A}$, and $\underline{f}$ is a six-dimensional vector-valued function. The equation (1) and other items to follow are written out in more explicit detail in paragraph 5.

3. Model

The assumed system model is represented by the pair of vector equations (all vectors are column vectors)

$$\dot{\underline{x}} = \underline{f}(\underline{x}) + \underline{u} \tag{2}$$

$$\underline{y}_k = H\underline{x}_k + \underline{v}_k$$

where

$\underline{x}$ is the 6-dimensional state vector

$\underline{y}_k$ is the 4-dimensional observation vector at time t_k

$\underline{u}$ is a 6-dimensional state noise vector with zero-mean, independent Gaussian samples and covariance matrix $P = E[u, u^T]$

$\underline{v}_k$ is a 6-dimensional observation noise vector with zero-mean, independent Gaussian samples and covariance matrix $M = E[v, v^T]$

H is a 4 x 6 matrix which transforms state coordinates to observation coordinates.

4. Recursion Algorithm

The Kalman filter recursion algorithm consists of a prediction and an estimation. The notation $\hat{\underline{x}}_{k/k-1}$ is used to denote the state vector estimate at time t_k based on all measurements through t_{k-1}. The prediction consists of predicting the state $\hat{\underline{x}}_{k/k-1}$ and its covariance matrix $S_{k/k-1}$ from the previous

estimates $\underline{\hat{x}}_{k-1/k-1}$, $S_{k-1/k-1}$ along with the equations of motion and their partial derivatives. The estimation consists of combining the predictions $\underline{\hat{x}}_{k/k-1}$, $S_{k/k-1}$ with the current measurement $\underline{y}_k$ to obtain the improved estimates $\underline{\hat{x}}_{k/k}$, $S_{k/k}$ valid at t_k, the time of the current measurement. This is described in more detail below.

a. Partial Derivatives

The required partial derivatives are indicated below in compact vector notation. They are presented more explicitly in paragraph 5 and in full detail in Appendix B.

Differentiating the equations of motion (1) with respect to time we obtain

$$\dot{\underline{x}} = \underline{f}(\underline{x})$$

$$\ddot{\underline{x}} = \frac{\partial \underline{f}}{\partial \underline{x}} \dot{\underline{x}} = \frac{\partial \underline{f}}{\partial \underline{x}} \underline{f}$$

$$\ddot{\underline{\hat{x}}}_{k/k-1} = A_k \underline{f}(\underline{\hat{x}}_{k/k-1}) \qquad (3)$$

where

$$A_k \equiv \frac{\partial \underline{f}}{\partial \underline{x}} \Bigg|_{\underline{x} = \underline{\hat{x}}_{k/k-1}}$$

Differentiating with respect to $\underline{x}_{k-1}$ we obtain

$$\dot{\underline{x}} = \underline{f}(\underline{x})$$

$$\frac{\partial}{\partial \underline{x}_{k-1}} \left(\frac{d\underline{x}}{dt}\right) = \frac{\partial \underline{f}}{\partial \underline{x}} \frac{\partial \underline{x}}{\partial \underline{x}_{k-1}}$$

$$\frac{d}{dt} \left(\frac{\partial \underline{x}}{\partial \underline{x}_{k-1}}\right) = \frac{\partial \underline{f}}{\partial \underline{x}} \frac{\partial \underline{x}}{\partial \underline{x}_{k-1}}$$

$$\dot{\phi}_k = A_k \phi_k \qquad (4)$$

where

$$\phi_k \equiv \phi(t_k, t_{k-1}) \equiv \frac{\partial \underline{x}_k}{\partial \underline{x}_{k-1}}$$

b. Prediction

Using (3) in a second order Taylor expansion we obtain the state vector prediction

$$\underline{\hat{x}}_{k/k-1} = \underline{\hat{x}}_{k-1/k-1} + \dot{\underline{\hat{x}}}_{k-1/k-1}\,\Delta t + \frac{1}{2}\ddot{\underline{\hat{x}}}_{k-1/k-1}\,\Delta t^2$$

$$= \underline{\hat{x}}_{k-1/k-1} + \underline{f}(\underline{\hat{x}}_{k-1/k-1})\,\Delta t + \frac{1}{2} A_{k-1}\,\underline{f}(\underline{\hat{x}}_{k-1/k-1})\,\Delta t^2 \quad (5)$$

or

$$\underline{\hat{x}}_{k/k-1} = \underline{\hat{x}}_{k-1/k-1} + \left[I + \frac{1}{2} A_{k-1}\,\Delta t\right] \underline{f}(\underline{\hat{x}}_{k-1/k-1})\,\Delta t \quad .$$

The covariance matrix of the state estimate is predicted as

$$S_{k/k-1} = \phi_k \left[S_{k-1/k-1} + P\Delta t\right] \phi_k^T \quad . \quad (6)$$

Using (4) in a first order Taylor expansion we obtain

$$\phi_k = \phi_{k-1} + \dot{\phi}_{k-1}\,\Delta t = \left[I + A_{k-1}\,\Delta t\right] \phi_{k-1} \quad .$$

Setting $\phi_{k-1} = I$ at each step the transition matrix ϕ_k required in (6) is computed as

$$\phi_k = I + A_{k-1}\,\Delta t \quad . \quad (7)$$

c. Estimation

The estimation algorithm follows.

$$\left.\begin{aligned} \underline{\hat{x}}_{k/k} &= \underline{\hat{x}}_{k/k-1} + W_k\,(\underline{y}_k - H\,\underline{\hat{x}}_{k/k-1}) \\ W_k &= S_{k/k-1}\,H^T\,(H\,S_{k/k-1}\,H^T + M)^{-1} \\ S_{k/k} &= (I - W_k\,H)\,S_{k/k-1}) \end{aligned}\right\} \quad (8)$$

where

$\underline{\hat{x}}_{k/k-1}$ is the state vector estimate at time t_k based on all measurements through time t_{k-1}.

$S_{k/k-1}$ is the covariance matrix (6 x 6) of the estimate $\underline{\hat{x}}_{k/k-1}$.

W_k is the weighting or gain matrix (6 x 4)

M is the (4 x 4) measurement noise covariance matrix $E[\underline{v}, \underline{v}^T]$.

The present implementation assumes that the measurement noise covariance M does not change with time. If later desired this restriction can be easily removed.

5. Vectors and Matrices

This paragraph contains some of the vectors and matrices used above in the more explicit and specialized form that they appear in the computer implementation.

$$\underline{y}_k = [R, E, A, \dot{R}]_k^T = \text{observation vector}$$

$$\underline{x} = [R, E, A, \dot{R}, \dot{E}, \dot{A}]^T = \text{state vector}$$

$$\underline{f}(\underline{x}) = [f_1(\underline{x}), f_2(\underline{x}), \ldots, f_6(\underline{x})]^T$$

$$= [\dot{R}, \dot{E}, \dot{A}, \ddot{R}(\underline{x}), \ddot{E}(\underline{x}), \ddot{A}(\underline{x})]^T$$

$$H = \begin{bmatrix} 1 & 0 & 0 & 0 & 0 & 0 \\ 0 & 1 & 0 & 0 & 0 & 0 \\ 0 & 0 & 1 & 0 & 0 & 0 \\ 0 & 0 & 0 & 1 & 0 & 0 \end{bmatrix}$$

$$M = \begin{bmatrix} \sigma_M^2(R) & 0 & 0 & 0 \\ 0 & \sigma_M^2(E) & 0 & 0 \\ 0 & 0 & \sigma_M^2(A) & 0 \\ 0 & 0 & 0 & \sigma_M^2(\dot{R}) \end{bmatrix}$$ = Measurement covariance

$$A = \begin{bmatrix} 0 & 0 & 0 & 1 & 0 & 0 \\ 0 & 0 & 0 & 0 & 1 & 0 \\ 0 & 0 & 0 & 0 & 0 & 1 \\ \frac{\partial \ddot{R}}{\partial R} & \frac{\partial \ddot{R}}{\partial E} & \frac{\partial \ddot{R}}{\partial A} & \frac{\partial \ddot{R}}{\partial \dot{R}} & \frac{\partial \ddot{R}}{\partial \dot{E}} & \frac{\partial \ddot{R}}{\partial \dot{A}} \\ \frac{\partial \ddot{E}}{\partial R} & \frac{\partial \ddot{E}}{\partial E} & \frac{\partial \ddot{E}}{\partial A} & \frac{\partial \ddot{E}}{\partial \dot{R}} & \frac{\partial \ddot{E}}{\partial \dot{E}} & \frac{\partial \ddot{E}}{\partial \dot{A}} \\ \frac{\partial \ddot{A}}{\partial R} & \frac{\partial \ddot{A}}{\partial E} & \frac{\partial \ddot{A}}{\partial A} & \frac{\partial \ddot{A}}{\partial \dot{R}} & \frac{\partial \ddot{A}}{\partial \dot{E}} & \frac{\partial \ddot{A}}{\partial \dot{A}} \end{bmatrix}$$ (See Appendix B)

$$\phi_k = I + A_{k-1}\,\Delta t = \text{transition matrix}$$

Note that the transition matrix ϕ_k is fully coupled except for linearization approximations.

The state driving noise matrix used is

$$P = \begin{bmatrix} 0 & 0 & 0 & 0 & 0 & 0 \\ 0 & 0 & 0 & 0 & 0 & 0 \\ 0 & 0 & 0 & 0 & 0 & 0 \\ 0 & 0 & 0 & \sigma_N^2(\dot{R}) & 0 & 0 \\ 0 & 0 & 0 & 0 & \sigma_N^2(\dot{E}) & 0 \\ 0 & 0 & 0 & 0 & 0 & \sigma_N^2(\dot{A}) \end{bmatrix}$$

The non-zero elements are computed from stored values of $\sigma_N^* = \sigma_N/\sqrt{10}$ according to data source as indicated below.

Data Source	$\sigma_N^*(\dot{R})$, m/s	$\sigma_N^*(\dot{E})$, μrad/s	$\sigma_N^*(\dot{A})$, μrad/s
Millstone	.01	.10	.10
Upper Visible	---	.01	.01
Lower Visible	---	.001	.001
IR	.0001	.001	.001

S is the 6 x 6 state estimate covariance matrix. The diagonal terms are the variances of the estimates.

$$S_{11} = \sigma^2(R) \qquad S_{22} = \sigma^2(E) \qquad S_{33} = \sigma^2(A)$$

$$S_{44} = \sigma^2(\dot{R}) \qquad S_{55} = \sigma^2(\dot{E}) \qquad S_{66} = \sigma^2(\dot{A})$$

The off-diagonal elements are symmetric and are the covariances of the estimates.

$S_{12} = \text{cov}(R,E)$ $S_{23} = \text{cov}(E,A)$ $S_{34} = \text{cov}(A,\dot{R})$ $S_{45} = \text{cov}(\dot{R},\dot{E})$ $S_{56} = (\dot{E},\dot{A})$

$S_{13} = \text{cov}(R,A)$ $S_{24} = \text{cov}(E,\dot{R})$ $S_{35} = \text{cov}(A,\dot{E})$ $S_{46} = \text{cov}(\dot{R},\dot{A})$

$S_{14} = \text{cov}(R,\dot{R})$ $S_{25} = \text{cov}(E,\dot{E})$ $S_{36} = \text{cov}(A,\dot{A})$

$S_{15} = \text{cov}(R,\dot{E})$ $S_{26} = \text{cov}(E,\dot{A})$

$S_{16} = \text{cov}(R,\dot{A})$

The lower triangular elements are set equal to their symmetric elements to save computation.

It is worth noting that, in the above, H takes on the particularly simple form indicated because the state variables are in the same coordinates as the observations. If this were not true H would become more complex. For example, if the state variables were expressed in radar-centered rectangular coordinates (x, y, z), the observations would be nonlinear functions of the state.

$$R = R(x, y, z)$$
$$E = E(x, y, z)$$
$$A = A(x, y, z)$$
$$\dot{R} = \dot{R}(x, y, z, \dot{x}, \dot{y}, \dot{z})$$

Linearization approximations would then be required and lead to the considerably more complex H below.

$$H = \begin{bmatrix} \frac{\partial R}{\partial x} & \frac{\partial R}{\partial y} & \frac{\partial R}{\partial z} & 0 & 0 & 0 \\ \frac{\partial E}{\partial x} & \frac{\partial E}{\partial y} & \frac{\partial E}{\partial z} & 0 & 0 & 0 \\ \frac{\partial A}{\partial x} & \frac{\partial A}{\partial y} & \frac{\partial A}{\partial z} & 0 & 0 & 0 \\ \frac{\partial \dot{R}}{\partial x} & \frac{\partial \dot{R}}{\partial y} & \frac{\partial \dot{R}}{\partial z} & \frac{\partial \dot{R}}{\partial \dot{x}} & \frac{\partial \dot{R}}{\partial \dot{y}} & \frac{\partial \dot{R}}{\partial \dot{z}} \end{bmatrix} \tag{9}$$

The indicated partials are written in full in Reference 2.

6. Data Editing

Dynamic data editing is performed by the filter. Data which deviate from predicted values by more than dynamically computed threshold values are tagged as bad and deleted from the estimation process. The threshold values are computed as

$$5\sigma + 2\sigma_M$$

where σ_M is the measurement accuracy for the particular sensor and σ is initially the *a priori* state vector accuracy and subsequently the dynamically computed state vector estimation accuracy. The pre-assigned accuracies are as indicated below.

	Sensor	R(m)	E(μr)	A(μr)	R(m/s)
$\sigma_{a\ priori}$	All	5,000	100,000	100,000	500
σ_M	IR	200	10	10	0.2
	UV		35	35	
	LV		20	20	
	MH	1,350	350	350	3.5

The action of the dynamic editing is to initially accept almost all data and to become more selective as the filter estimates improve with track length. Initially, $\sigma = \sigma_{a\ priori}$ and is large compared to σ_M so that threshold values are approximately 5 $\sigma_{a\ priori}$. After a few seconds of track, σ becomes small compared to σ_M, so that the threshold values become approximately 2 σ_M. For example, lower visible data are initially edited with a threshold of approximately 500,000 μrad and, after a long track, with a threshold of approximately 40 μrad.

IV. SOME RESULTS

The Firepond Kalman filter reported here was initially implemented with Millstone data and later with Firepond visible and IR data. In this section we present some results for two satellite track missions which indicate the kind of results obtained with lower visible and IR Doppler data.

1. Mission 76079.0036

This was a Kalman track with lower visible angles only on object 5398 (LCS4) performed on 18 March 1976. The tracking crew consisted of L. Swezey, R. Capes, and S. Catalano. This was a fifteen minute satellite pass with peak elevation of 48.3°. The object was acquired at 8° above the horizon, put into Kalman directing mode at 25° ascending, and held in the lower TV reticle down to 8° for about nine minutes. The scan and transit time servos were on but the incremental refraction servo was not operational and left off.

A post-mission orbit fit was done on about 8.5 minutes of the lower visible angles with star calibration corrections applied. Kalman angle estimates were within ± 30 μrad of the orbit values. To minimize the effect of not having applied incremental refraction corrections to the visible angle data, the orbit fit was repeated with only the data above 40° elevation (about three minutes of data) where incremental refraction errors are less than 7 μrad. the Kalman angle estimates now agreed with orbit values to within about ± 7.5 μrad in azimuth and ± 5.0 μrad in elevation. Figures 2a and 2b show the corrected lower visible angle observations fed to the filter and the corresponding Kalman estimates. Zero levels represent the fitted orbit values. These results do not preclude the possibility of linear biases in the system since the orbit fit would adjust to such biases over this short an orbital excursion.

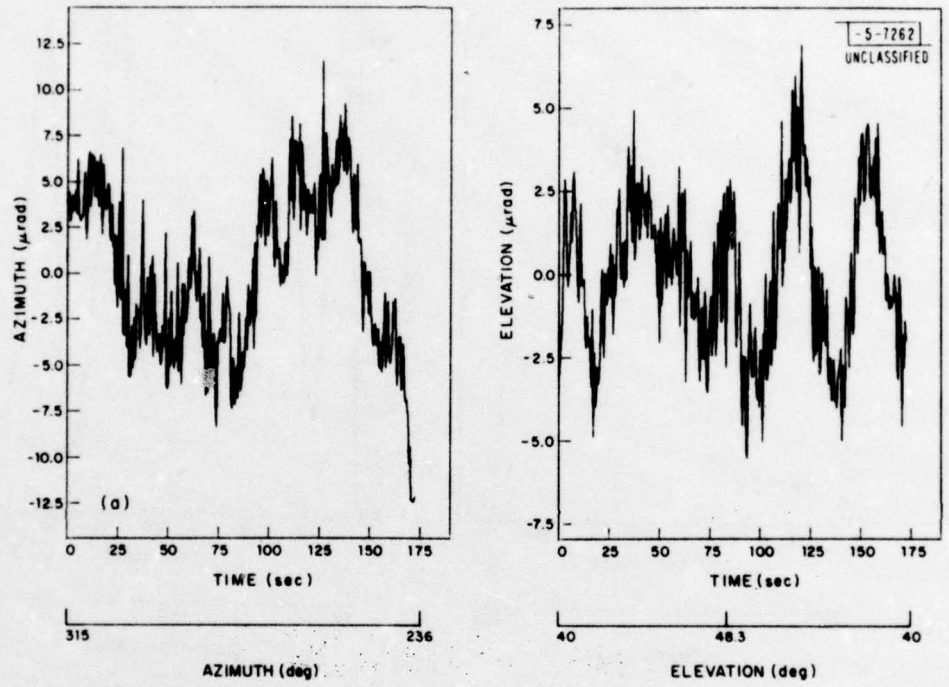

Fig. 2a. Data Residuals (Orbit fit - LV observations), 76079.0036, LCS-4.

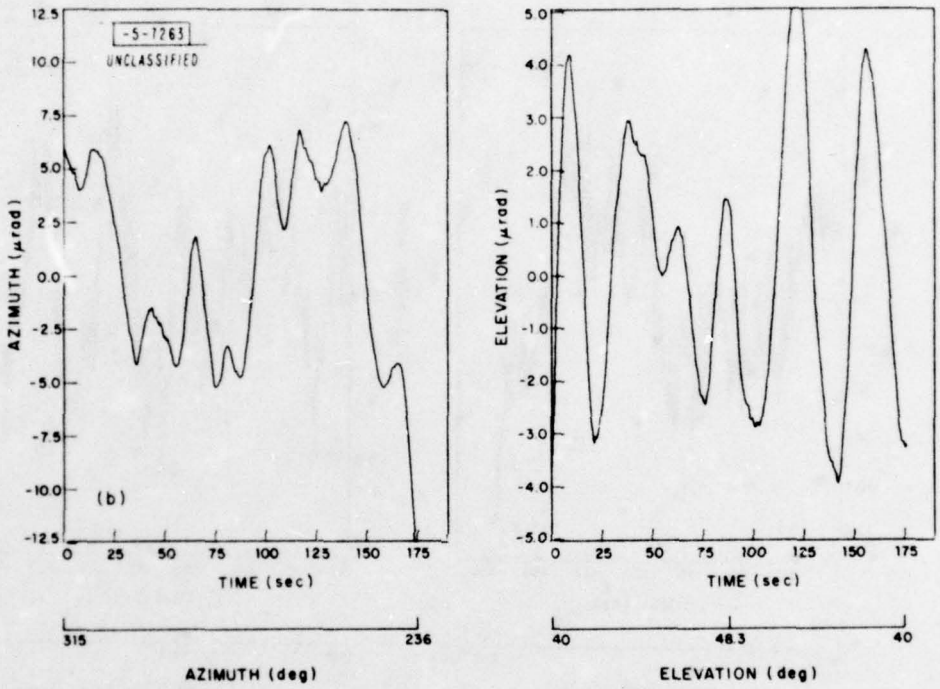

Fig. 2b. Estimate Residuals (Orbit fit - Kalman estimates), 76079.0036, LCS-4.

2. Mission 76098.0011

This was a Kalman track using lower visible angles and IR Doppler and was performed on GEOS-III on 7 April 1976. It was a 14 minute pass with peak elevation of 63.8°. The tracking crew consisted of R. Capes, L.DiPalma, J. Linder, R. McPherson, L. Swezey, and R. Teoste. The object was acquired in lower visible angles from nominals and by about 32° elevation (going up) the filter was in good track with this angles-only data. At about 41° IR Doppler hits commenced, initially intermittent and later steady. The filter immediately accepted these and continued the track with this IR Doppler data in addition to the lower visible data. At about 54°, the mount was put in Kalman directing mode and remained in this mode to the end of the pass, holding the IR beam on the object through peak elevation, down to about 28° elevation, with long duration IR Doppler returns for about four minutes in essentially "hands off" mode.

An orbit fit was performed on the basis of the angle and Doppler measurements. Figures 3a and 3b show the Kalman observations and estimates relative to the fitted orbit. All measurements include corrections for servo errors (scan, transit time, and incremental refraction), angle and Doppler tracker errors, and star calibration misalignments. The azimuth residuals are contained within a spread of about 50 μrad while the elevation residuals are contained within a spread of about 100 μrad. Some of the funny shapes of these curves are probably due to the star calibration corrections which were still in the process of being improved. The Doppler residuals are contained within a spread of about 0.5 m/s. The discontinuity of about 0.2 m/s occurs at peak elevation and was probably due to a system bias.

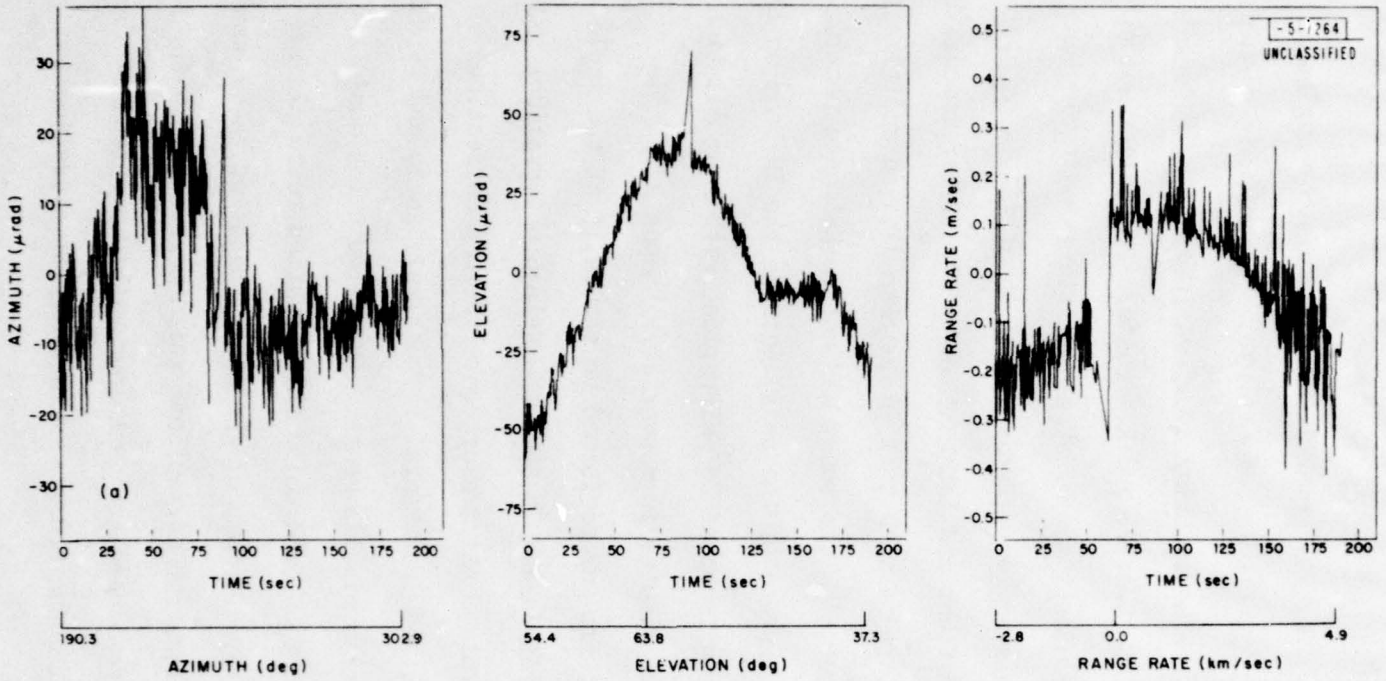

Fig. 3a. Data Residuals (Orbit fit - LV/IR-Doppler observations), 76098.0011, GEOS-3.

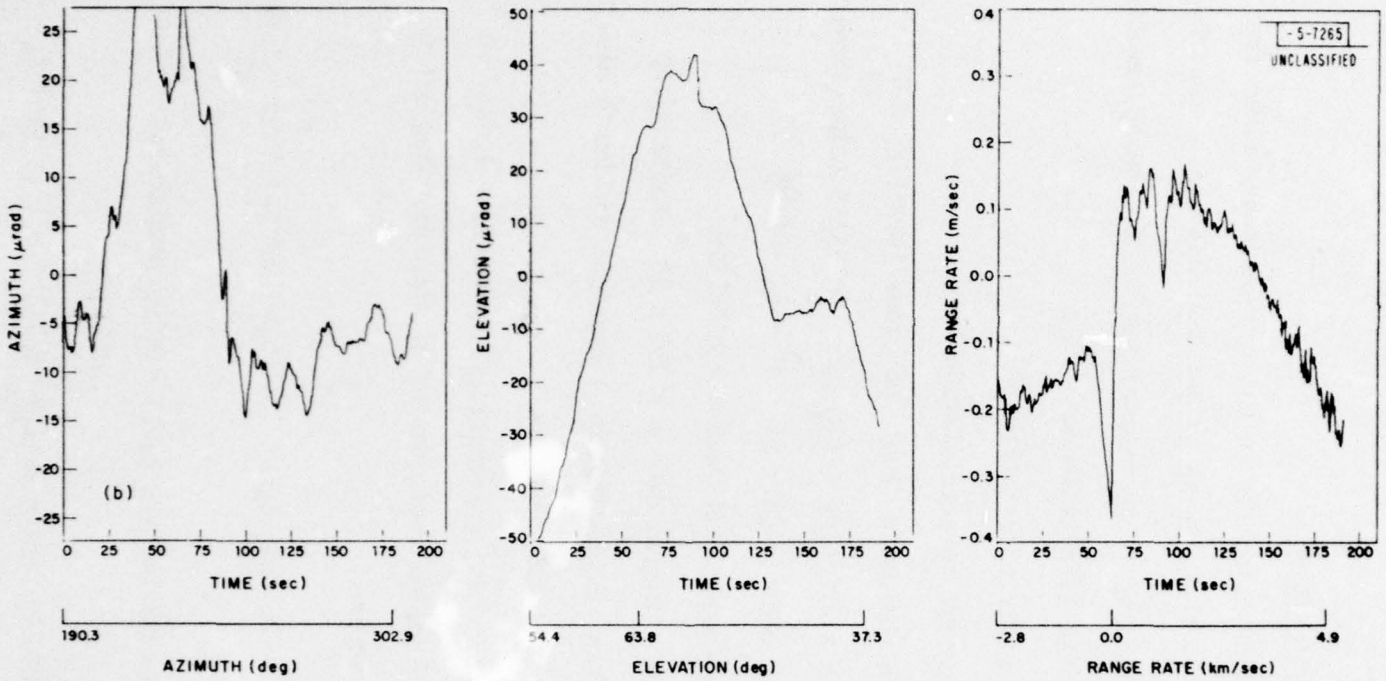

Fig. 3b. Estimate Residuals (Orbit fit-Kalman estimates), 76098.0011, GEOS-3.

APPENDIX A

Equations of Motion

The equations of motion in this appendix are taken from Reference 3 with the drag terms (containing ρ) deleted. An ellipsoidal Earth (equatorial radius a and flattening f) is assumed and the following symbols are used.

μ = geodetic site latitude

μ_c = geocentric site latitude

ϕ = geocentric target latitude

R_c = Earth radius to "foot" of radar (see Fig. A-1)

f = Earth flattening = $\frac{1}{298.25}$ = .00335289 (dimensionless)

e = Earth eccentricity [$1 - e^2 = (1 - f)^2$]

a = Earth equatorial radius = 6378145m

ω = Earth rotation rate = 7.292×10^{-5} radians/sec

GM = product of gravitational constant and Earth mass = 3.985768×10^{14} m^3/sec^2

J = Earth second gravitational harmonic = 1.62×10^{-3} (dimensionless)

The equations of motion then consist of the following set of three coupled differential equations.

$$\ddot{R}=R(\dot{E}^2+\dot{A}^2\cos^2E) - 2\omega(\xi_E V_A-\xi_A V_E) - \omega^2(\xi_R r \sin\phi-r_R) + \frac{g_r r_R}{r} + g_\xi \xi_R$$

$$\ddot{E}=\frac{-1}{R}\{2\dot{R}\dot{E}+R\dot{A}^2\sin E\cos E+2\omega(\xi_A V_R-\xi_R V_A) + \omega^2(\xi_E r \sin\phi-r_E) - \frac{g_r r_E}{r} - g_\xi \xi_E\}$$

$$\ddot{A}=\frac{-1}{R\cos E}\{2(\dot{R}A\cos E-\dot{R}\dot{A}\sin E) + 2\omega(\xi_R V_E-\xi_E V_R) + \omega^2(\xi_A r \sin\phi-r_A) - \frac{g_r r_A}{r} - g_\xi \xi_A\}$$

where

$$\xi_R = \cos\mu \cos E \cos A + \sin\mu \sin E$$

$$\xi_E = -\cos\mu \sin E \cos A + \sin\mu \cos E$$

$$\xi_A = -\cos\mu \sin A$$

$$V_R = \dot{R},\ V_E = R\dot{E},\ V_A = R\dot{A}\cos E$$

$$V = \{V_R^2 + V_E^2 + V_A^2\}^{1/2}$$

$$r_R = R + Q_1 R_c \sin E - Q_2 R_c \cos E \cos A$$

$$r_E = Q_1 R_c \cos E + Q_2 R_c \sin E \cos A$$

$$r_A = Q_2 R_c \sin A$$

$$Q_1 = \cos(\mu - \mu_c) + H/R_c$$

$$Q_2 = \sin(\mu - \mu_c)$$

$$r = R_c\{(R/R_c)^2 + 2(R/R_c)(Q_1 \sin E - Q_2 \cos E \cos A) + Q_1^2 + Q_2^2\}^{1/2}$$

$$g_r = \frac{-GM}{r^2}\{1 + J(\frac{a}{r})^2 (1 - 5\sin^2\phi\}$$

$$g_\xi = \frac{-2GM}{r^2} J(\frac{a}{r})^2 \sin\phi$$

$$\sin\phi = \frac{1}{r}\{R\cos E \cos A \cos\mu + (H + R\sin E)\sin\mu + R_c \sin\mu_c\}$$

$$R_c = \left[\frac{a^2(1 - e^2)}{1 - e^2\cos^2\mu_c}\right]^{\frac{1}{2}} = a(1 - f)\,[1 - f(2 - f)\cos^2\mu_c]^{-1/2}$$

$$\mu_c = \tan^{-1}[(1 - e^2)\tan\mu]$$

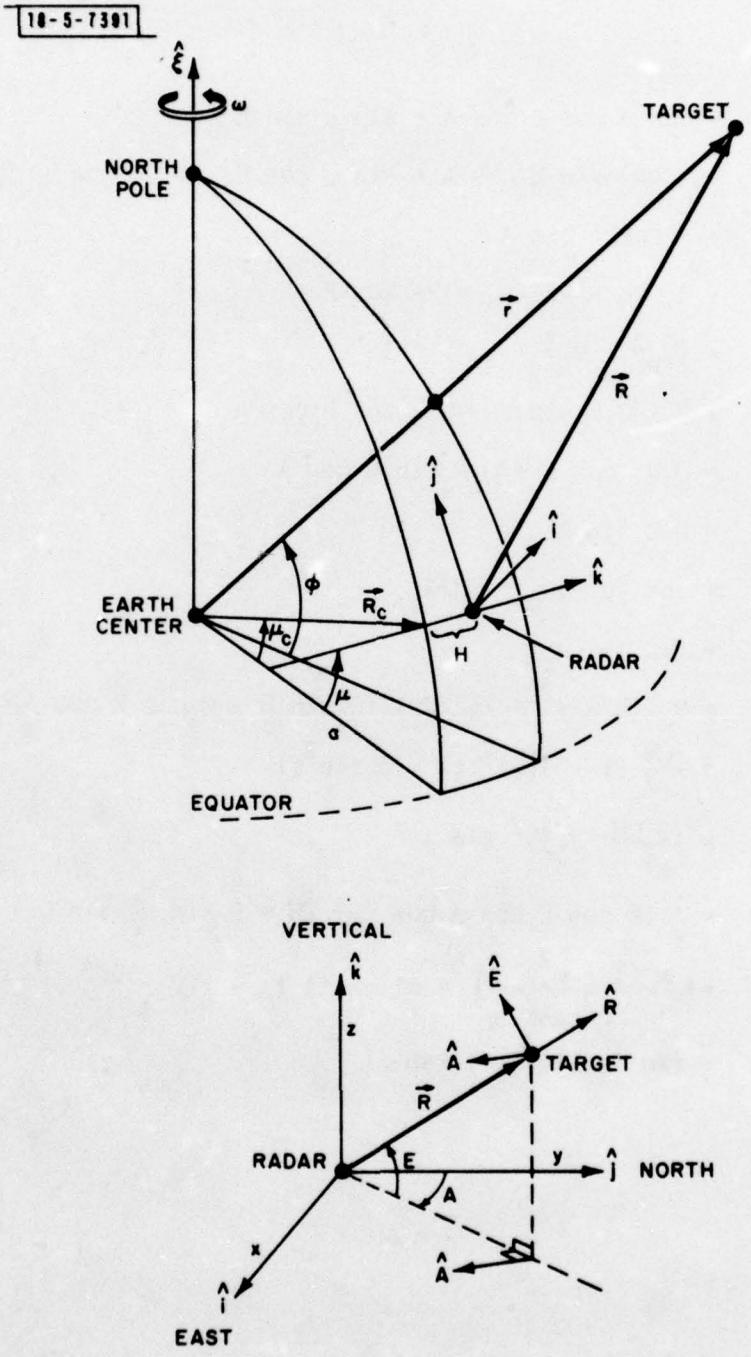

Fig. A-1. Earth-Sensor-Target Geometry.

APPENDIX B

Partial Derivatives

This section presents in full detail the A-matrix partials indicated in paragraph 5. The elements of the upper half A-matrix are trivial and already shown. Therefore, only the lower half A-matrix elements are presented here. The notation of Appendix A is adhered to and the ellipsoidal Earth model is retained.

The following auxiliary partials are first required.

$$\frac{\partial r_R}{\partial E} = R_c(Q_1 \cos E + Q_2 \sin E \cos A), \qquad \frac{\partial r_R}{\partial A} = R_c Q_2 \cos E \sin A$$

$$\frac{\partial r_E}{\partial E} = -R_c(Q_1 \sin E - Q_2 \cos E \cos A), \qquad \frac{\partial r_E}{\partial A} = -R_c Q_2 \sin E \sin A$$

$$\frac{\partial r_A}{\partial A} = R_c Q_2 \cos A \quad .$$

Utilizing these auxiliary partials, the lower half A-matrix partials are as indicated below.

$$A_{41} \equiv \frac{\partial \ddot{R}}{\partial R} = \frac{V_E^2 + V_A^2}{R^2} + 2\frac{\omega}{R}(\xi_A V_E - \xi_E V_A) - \omega^2(\xi_R^2 - 1) + \frac{GM}{r^3}\left[3\left(\frac{r_R}{r}\right)^2 - 1\right] \quad .$$

$$A_{42} \equiv \frac{\partial \ddot{R}}{\partial E} = -2k\dot{A}^2 \sin E \cos E + 2\omega R\dot{A} \left(\xi_E \sin E + \xi_R \cos E\right)$$

$$- \omega^2 \left[\xi_E \left(R\xi_R + r \sin\phi\right) - \frac{\partial r_R}{\partial E}\right]$$

$$+ \frac{GM}{r^3}\left[3\left(\frac{r_R}{r}\right)\left(\frac{r_E}{r}\right) R - \frac{\partial r_R}{\partial E}\right]$$

$$A_{43} \equiv \frac{\partial \ddot{R}}{\partial \dot{A}} = 2\omega\left(\xi_A V_A \sin E - V_E \cos\mu \cos A\right)$$

$$- \omega^2 \left[\xi_A \cos E \left(R\xi_R + r \sin\phi\right) - \frac{\partial r_R}{\partial A}\right]$$

$$+ \frac{GM}{r^3}\left[3\left(\frac{r_R}{r}\right)\left(\frac{r_A}{r}\right) R \cos E - \frac{\partial r_R}{\partial A}\right]$$

$$A_{44} \equiv \frac{\partial \ddot{R}}{\partial \dot{R}} = 0$$

$$A_{45} \equiv \frac{\partial \ddot{R}}{\partial \dot{E}} = 2\left(V_E + \omega R\xi_A\right)$$

$$A_{46} \equiv \frac{\partial \ddot{R}}{\partial \dot{A}} = 2 \cos E \left(V_A - \omega R\xi_E\right)$$

$$A_{51} \equiv \frac{\partial \ddot{E}}{\partial R} = 2\frac{V_R}{R^2}(\dot{E} + \omega\xi_A) - \frac{\omega^2}{R}\left[\xi_R\xi_E - \frac{1}{R}(\xi_E\, r\sin\phi - r_E)\right]$$

$$+ \frac{GM}{r^3}\frac{1}{R}\left[3\left(\frac{r_E}{r}\right)\left(\frac{r_R}{r}\right) + \left(\frac{r_E}{R}\right)\right]$$

$$A_{52} \equiv \frac{\partial \ddot{E}}{\partial E} = \dot{A}^2(1 - 2\cos^2 E) + 2\omega\dot{A}(\xi_E \cos E - \xi_R \sin E)$$

$$- \frac{\omega^2}{R}\left[\xi_E^2 R - \xi_R\, r\sin\phi - \frac{\partial r_E}{\partial E}\right]$$

$$+ \frac{GM}{r^3}\left[3\left(\frac{r_E}{r}\right)^2 - \frac{1}{R}\frac{\partial r_E}{\partial E}\right]$$

$$A_{53} \equiv \frac{\partial \ddot{E}}{\partial A} = 2\frac{\omega}{R}\left[V_R \cos\mu \cos A + V_A\, \xi_A \cos E\right]$$

$$- \frac{\omega^2}{R}\left[\xi_A\ (\xi_E R\cos E - r\sin\phi \sin E) - \frac{\partial r_E}{\partial A}\right]$$

$$+ \frac{GM}{r^3}\frac{1}{R}\left[3\left(\frac{r_E}{r}\right)\left(\frac{r_A}{r}\right) R\cos E - \frac{\partial r_E}{\partial A}\right]$$

$$A_{54} \equiv \frac{\partial \ddot{E}}{\partial \dot{R}} = -\frac{2}{R}(\dot{E} + \omega\xi_A)$$

$$A_{55} \equiv \frac{\partial \ddot{E}}{\partial \dot{E}} = -2\frac{V_R}{R}$$

$$A_{56} \equiv \frac{\partial \ddot{E}}{\partial \dot{A}} = -2\cos E(\dot{A}\sin E - \omega\xi_R)$$

$$A_{61} \equiv \frac{\partial \ddot{A}}{\partial R} = 2\frac{V_R}{R^2}\left(\dot{A} - \frac{\omega\xi_E}{\cos E}\right) - \frac{\omega^2}{R^2\cos E}\left[\xi_A(\xi_R R - r\sin\phi) + r_A\right]$$

$$+ \frac{GM}{r^3}\frac{1}{R\cos E}\left[3\left(\frac{r_A}{r}\right)\left(\frac{r_R}{r}\right) + \left(\frac{r_A}{R}\right)\right]$$

$$A_{62} \equiv \frac{\partial \ddot{A}}{\partial E} = \frac{2\dot{A}\dot{E}}{\cos^2 E} - \frac{2\omega}{R\cos^2 E}\left(V_E \sin\mu + V_R \cos\mu \cos A\right)$$

$$- \frac{\omega^2}{R\cos^2 E}\left[\xi_E\xi_A R\cos E + (\xi_A r\sin\phi - r_A)\sin E\right]$$

$$+ \frac{GM}{r^3}\frac{1}{\cos E}\left[3\left(\frac{r_E}{r}\right)\left(\frac{r_A}{r}\right) - \left(\frac{r_A}{R}\right)\tan E\right]$$

$$A_{63} \equiv \frac{\partial \ddot{A}}{\partial A} = -\frac{2\omega\xi_A}{R\cos E}\left(V_E \cos E + V_R \sin E\right)$$

$$- \frac{\omega^2}{R\cos E}\left[\xi_A^2 R\cos E - r\sin\phi\cos\mu\cos A + \frac{\partial r_A}{\partial A}\right]$$

$$+ \frac{GM}{r^3}\left[3\left(\frac{r_A}{r}\right)^2 - \frac{1}{R\cos E}\frac{\partial r_A}{\partial A}\right]$$

$$A_{64} \equiv \frac{\partial \ddot{A}}{\partial \dot{E}} = -\frac{2}{R\cos E}\left(\dot{A}\cos E - \omega\xi_E\right)$$

$$A_{65} \equiv \frac{\partial \ddot{A}}{\partial \dot{E}} = \frac{2}{\cos E}\left(\dot{A}\sin E - \omega\xi_R\right)$$

$$A_{66} \equiv \frac{\partial \ddot{A}}{\partial \dot{A}} = 2\left(\dot{E}\tan E - \frac{V_R}{R}\right)$$

APPENDIX C

Serial Estimation

At this point it is convenient to drop the double subscript notation of the estimation algorithm (8) and re-write it as

$$\left.\begin{aligned} W &= S(-)H^T[H\,S(-)H^T + M]^{-1} \\ x(+) &= x(-) + W[y - H\,x(-)] \\ S(+) &= S(-) - W\,H\,S(-) \end{aligned}\right\} \qquad (1)$$

The first of the above equations requires the inversion of a 4 x 4 matrix. Many matrix inversion schemes have been proposed and used. Originally, the Firepond Kalman filter used an extended (for doppler) version of the scheme suggested in Reference 1 which involves inversion after factorization into diagonal matrices. This worked but was cumbersome in many respects. For example, if one or more components of the observation vector were missing, it was necessary to insert fictitious components with very low weights so as to make their effect insignificant. The assigning of these low weights then became a source of concern as to whether they would result in an ill-conditioned matrix that might behave badly upon inversion. Another approach might have been to reformulate the algorithm for each specific situation (i.e., 3 x 3 inversion for one missing component, etc.). This seemed even more awkward.

The technique* that is currently used avoids the above difficulties. It consists in regarding the four simultaneously occurring components of the observation vector as having occurred serially over a time interval $\Delta t = 0$. Then instead of one pass through the algorithm (1), requiring inversion of a

*First suggested to the author in Reference 4, p. 304, 305.

4 x 4 matrix, a pass is made for each observation component, each pass requiring only the trivial inversion of a 1 x 1 matrix. More explicitly four passes are made through the algorithm with y, H, and M as indicated below.

1. $y = R$, $H = [1, 0, 0, 0, 0, 0]$, $M = \sigma_M^2(R)$
2. $y = E$, $H = [0, 1, 0, 0, 0, 0]$, $M = \sigma_M^2(E)$
3. $y = A$, $H = [0, 0, 1, 0, 0, 0]$, $M = \sigma_M^2(A)$
4. $y = \dot{R}$, $H = [0, 0, 0, 1, 0, 0]$, $M = \sigma_M^2(\dot{R})$

If an observation component is missing or bad, the pass for that component is merely omitted. Each pass results in a six dimensional column weight vector W which is applied to the old state vector x(-) and covariance matrix S(-) to obtain the new ones, x(+), S(+). On the pass for the next observation component, the new x(+), S(+) replace the old x(-), S(-).

A simplified version of the FORTRAN code for processing four simultaneously occurring observation components through the algorithm (1), in the described serial estimation mode, is shown below. The indicated FORTRAN array allocation is assumed.

x(6) = { x(-) on entry = predicted state at observation time
       { x(+) on exit = estimated state at observation time

y(4) = y, observation vector

D(4) = Data flags array, one flag for each component of y, with a flag of 1 for observations which are to be included in the estimation.

SIGMA(4) = $\sigma_M(y_i)$ = assumed measurement accuracies (standard deviations)

SP (6, 6) = S(+), the new covariance matrix

SM (6, 6) = S(-), the old covariance matrix

```
      DO 30  K = 1, 4
      RES = Y(K) - X(K)
      IF (D(K) .NE. 1) GO TO 30
      TERM = 1.DO/(SM(K, K) + SIGMA (K)**2)
      DO 10 I = 1, 6
      W = SM(I, K)*TERM
      X(I) = X(I) + W*RES
      DO 10  J = 1, 6
10    SP(I, J) = SM(I, J) - W*SM(K, J)
      DO 20  M = 1, 6
      DO 20  N = 1, 6
20    SM(M, N) = SP(M, N)
30    CONTINUE
```

The above code is for illustration only. The actual FIREPOND implementation is close to the above but includes modifications which improve the computational speed (e.g., taking advantage of the symmetry of the covariance matrix).

The serial estimation implementation of (1) gives the same answers as the originally used 4 x 4 matrix inversion approach. However, the serial estimation approach is superior on several counts.

1. It does not require a literature search for the best matrix inversion scheme.
2. It requires less storage. The above code is very compact and no storage is required for a matrix inversion routine.
3. It is considerably easier to implement and more flexible in the

handling of missing or bad observation components.

4. It is computationally faster. This is due to the use of radar polar coordinates, since in these coordinates the matrix H takes on a particularly simple form (and in fact does not even appear in the above code). However, in other coordinates, H takes on the complex form (9) which would add considerably to the computation.

Appendix D

Pre-smoothing Algorithm

The pre-smoothing algorithm used here is that due to N. Levine reported in reference 5. As used herein, it performs recursive linear least squares smoothing on equally-spaced, equally-weighted data (with possible missing points) and gives estimates of position and velocity valid at the last data point. The algorithm is outlined below.

The following definitions are used:

x_n = the nth observation

$\hat{x}_n$ = its predicted value based on previous n-1 observations

$\bar{x}_n$ = its estimate after n observations

w_n = 1 for a good data point and 0 for a bad or missing data point

$\mu = \dot{x}\tau$ where τ is the constant data interval

$\hat{\mu}_n$ = predicted value of μ_n based on n - 1 observations

$\bar{\mu}_n$ = estimated value of μ_n based on n observations

Mathematically the algorithm can be written as follows:

Initial conditions: $F_1 = w_1$, $G_1 = H_1 = J_1 = 0$

$$\hat{x}_1 = x_1, \quad \hat{\mu}_1 = 0$$

Recursion ($n > 1$):

$$F_n = F_{n-1} + w_n$$

$$G_n = G_{n-1} + F_{n-1}$$

$$H_n = H_{n-1} + 2G_{n-1} + F_{n-1}$$

$$J_n = J_{n-1} + w_n H_n$$

$$\alpha_n = w_n H_n/J_n, \quad \beta_n = w_n G_n/J_n$$

$$\hat{x}_n = \bar{x}_{n-1} + \bar{\mu}_{n-1}, \quad \hat{\mu}_n = \bar{\mu}_{n-1}$$

$$\bar{x}_n = \hat{x}_n + \alpha_n (x_n - \hat{x}_n)$$

$$\bar{\mu}_n = \hat{\mu}_n + \beta_n (x_n - \hat{x}_n)$$

Program-wise, the computation is more efficiently organized as indicated below where the notation $A \leftarrow B$ means A is replaced by B.

Initial conditions: $F_1 = w_1$, $G_1 = H_1 = J_1 = 0$

$$\bar{x}_1 = x_1, \quad \bar{\mu}_1 = 0$$

Recursion (done in the indicated order):

$$H_n \leftarrow H_n + 2G_n + F_n$$

$$G_n \leftarrow G_n + F_n$$

$$F_n \leftarrow F_n + w_n$$

$$J_n \leftarrow J_n + w_n H_n$$

$$\bar{x}_n \leftarrow \bar{x}_n + \bar{\mu}_n$$

$$\Delta\bar{x}_n \leftarrow (x_n - \bar{x}_n)$$

$$\bar{x}_n \leftarrow \bar{x}_n + w_n \, \Delta\bar{x}_n \, H_n/J_n$$

$$\bar{\mu}_n \leftarrow \bar{\mu}_n + w_n \, \Delta\bar{x}_n \, G_n/J_n$$

In this form previous values can share the same locations as present values. All subscripts are therefore the same and can in fact be dropped. The quantity $\Delta\bar{x}_n$ is the difference between observed and predicted value. If it exceeds certain thresholds (90 km, 500 m/s, 10^o for range, doppler, and angle, respectively) the corresponding observation is deleted from the smoothing process and in effect replaced by its predicted value by setting $\Delta\bar{x}_n = 0$ in the last two steps above. This editing is intended to guard against gross glitch-type errors in the data. A count of the number of good observations in the tenth second smoothing process is maintained.

APPENDIX E

Millstone Doppler Coordinate Correction

Millstone range rate $\dot{R}_M$ is converted to Firepond-referenced range rate $\dot{R}$ as indicated below. Referring to the figure, let $\hat{R}$, $\hat{E}$, $\hat{A}$ be Firepond radar polar unit vectors. Then by vector definitions we have:

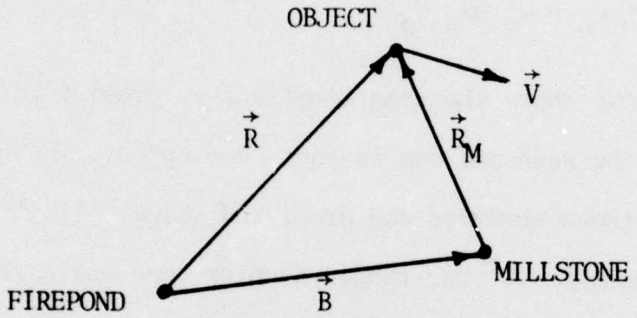

$$\vec{R} = R\hat{R}$$

$$\vec{B} = B_R\hat{R} + B_E\hat{E} + B_A\hat{A}$$

$$\vec{V} = V_R\hat{R} + V_E\hat{E} + V_A\hat{A}$$

$$\vec{R}_M = \vec{R} - \vec{B}$$

$$= (R - B_R)\,\hat{R} - B_E\hat{E} - B_A\hat{A}$$

Since $\dot{R}_M = \dfrac{\vec{V} \cdot \vec{R}_M}{\left|\vec{R}_M\right|}$, we have

$$\dot{R}_M = \frac{1}{R_M}\left[V_R\,(R - B_R) - V_E B_E - V_A B_A\right] .$$

Noting that $V_R = \dot{R}$, the Firepond-referenced range rate, and solving, we get

$$\dot{R} = \frac{R_M\dot{R}_M + B_E V_E + B_A V_A}{R - B_R}$$

In the above $V_E = R\dot{E}$, $V_A = R\dot{A}\cos E$. The required angle rates $\dot{E}$, $\dot{A}$ are taken as the Kalman filter Firepond-referenced angle rate estimates. The baseline vector $\vec{B}$ is the translation vector of Section II-2 with Firepond rectangular components in meters known as:

$$B_X = 117.000, \qquad B_Y = -15.098, \qquad B_Z = 16.901 \quad .$$

The required baseline components in radar-polar coordinates are obtained as:

$$B_R = B_X \cos E \sin A + B_Y \cos E \cos A + B_Z \sin E$$

$$B_E = -B_X \sin E \sin A - B_Y \sin E \cos A + B_Z \cos E$$

$$B_A = B_X \cos A - B_Y \sin A \quad .$$

R, E, A are the Firepond-referenced Millstone measurements R_M, E_M, A_M.

ACKNOWLEDGMENTS

The author wishes to thank R. Teoste for many helpful discussions and suggestions on several aspects of the filter, J. L. Nimmo for expert assistance in the implementation of the filter onto the Firepond real time program, R. N. Capes and L. W. Swezey for great skill, patience, and tenacity in coping with the many problems of bringing together a complex system for repeated tracking attempts at uncomfortable hours, and J. J. Alves for help with the post-mission data analysis programs. Thanks are also due to K. Miles and C. Willis for typing initial drafts of parts of the report and M. Ampolo and D. Brown for typing the final report.

REFERENCES

1. M. Gruber, "REDD System Tracking Filters," private communication.

2. M. Gruber, "An Approach to Target Tracking," Technical Note 1967-8, Lincoln Laboratory, M.I.T. (10 February 1967), DDC AD-654272.

3. S. F. Catalano, "Trajectory Equations of Motion in Radar Polar Corrdinates," Technical Note 1967-25, Lincoln Laboratory, M.I.T. (24 May 1967), DDC AD-652841.

4. Technical Staff, The Analytic Sciences Corporation, edited by Arthur Gelb, in "Applied Optimal Estimation," (M.I.T. Press, Cambridge, 14 January 1974).

5. N. Levine. "Recursive Least Squares Data Smoothing," The Bell System Technical Journal, 821-840 (May, 1961).

UNCLASSIFIED

SECURITY CLASSIFICATION OF THIS PAGE *(When Data Entered)*

REPORT DOCUMENTATION PAGE

READ INSTRUCTIONS BEFORE COMPLETING FORM

1. REPORT NUMBER: ESD-TR-77-42
2. GOVT ACCESSION NO.:
3. RECIPIENT'S CATALOG NUMBER:
4. TITLE *(and Subtitle)*: The Firepond Kalman Filter
5. TYPE OF REPORT & PERIOD COVERED: Technical Note
6. PERFORMING ORG. REPORT NUMBER: Technical Note 1977-10
7. AUTHOR(s): Sebastian F. Catalano
8. CONTRACT OR GRANT NUMBER(s): F19628-76-C-0002
9. PERFORMING ORGANIZATION NAME AND ADDRESS:
Lincoln Laboratory, M.I.T.
P.O. Box 73
Lexington, MA 02173
10. PROGRAM ELEMENT, PROJECT, TASK AREA & WORK UNIT NUMBERS:
ARPA Order 600
Program Element No. 62301E
Project No. 7E20
11. CONTROLLING OFFICE NAME AND ADDRESS:
Defense Advanced Research Projects Agency
1400 Wilson Boulevard
Arlington, VA 22209
12. REPORT DATE: 4 February 1977
13. NUMBER OF PAGES: 45 pp.
14. MONITORING AGENCY NAME & ADDRESS *(if different from Controlling Office)*:
Electronic Systems Division
Hanscom AFB
Bedford, MA 01731
15. SECURITY CLASS. *(of this report)*: Unclassified
15a. DECLASSIFICATION DOWNGRADING SCHEDULE:
16. DISTRIBUTION STATEMENT *(of this Report)*:
Approved for public release; distribution unlimited.
17. DISTRIBUTION STATEMENT *(of the abstract entered in Block 20, if different from Report)*:
18. SUPPLEMENTARY NOTES:
None
19. KEY WORDS *(Continue on reverse side if necessary and identify by block number)*:
Kalman filter
satellite tracking
Millstone radar
radar observations
20. ABSTRACT *(Continue on reverse side if necessary and identify by block number)*:

This report describes the satellite tracking Kalman filter implemented at the M.I.T. Lincoln Laboratory Firepond Infrared Research Facility at Westford, MA. The filter estimates a six dimensional state vector for mount direction from satellite observations. These observations can consist of range, elevation, azimuth, and range rate; and under push-button control, can be selected from among the available Firepond detectors (IR and optical) and the Millstone radar across the road.

Radar polar coordinates are used throughout and, in particular, both the estimates and the equations of motion are in these coordinates. The filter is fully coupled in the sense that every measurement improves every estimate. For example, angle measurements improve range and Doppler estimates, and conversely. Serial processing of simultaneous measurements is employed. This eliminates the need for matrix inversion, facilitates handling of missing data points, requires less storage, and is computationally faster.

A detailed mathematical description of the filter is included along with some typical satellite tracking results.

DD FORM 1 JAN 73 1473 EDITION OF 1 NOV 65 IS OBSOLETE

UNCLASSIFIED

SECURITY CLASSIFICATION OF THIS PAGE *(When Data Entered)*

207650 only